DYNLO: Enhancing Non-Linear Regularized State Observer Brain Mapping Technique by Parameter Estimation with Extended Kalman Filter

A.F. Soler[1], E. Giraldo[2], M. Molinas[1]

[1] Norwegian University of Science and Technology, Trondheim, Norway
{andres.f.soler.guevara, marta.molinas}@ntnu.no
[2] Universidad Tecnológica de Pereira, Pereira, Colombia
egiraldos@utp.edu.co

Abstract. The underlying activity in the brain can be estimated using methods based on discrete physiological models of the neural activity. These models involve parameters for weighting the estimated source activity of previous samples, however, those parameters are subject- and task-dependent. This paper introduces a dynamical non-linear regularized observer (DYNLO), through the implementation of an Extended Kalman Filter (EKF) for estimating the model parameters of the dynamical source activity over the neural activity reconstruction performed by a non-linear regularized observer (NLO). The proposed methodology has been evaluated on real EEG signals using a realistic head model. The results have been compared with least squares (LS) for model parameter estimation with NLO and the multiple sparse prior (MSP) algorithm for source estimation. The correlation coefficient and relative error between the original EEG and the estimated EEG from the source reconstruction were inspected and the results show an improvement of the solution in terms of the aforementioned measurements and a reduction of the computational time.

Keywords: EEG-based Brain Mapping, Extended Kalman Filter EKF, Non-Linear Regularized Observer NLO, Dynamic Inverse Solution

1 Introduction

Electroencephalography (EEG) is a non-invasive technique for recording information of the electrical activity in the brain through the measurement of electrical potentials using electrodes in the scalp. The signals contain information with a high temporal resolution and the analysis of the data has become a useful tool to diagnose different forms of brain disorders like Epilepsy, Parkinson, sleep or memory disorders. In addition, the EEG information can be used to identify the localization of the neural activity in the brain through the use of brain mapping techniques. Nevertheless, the inverse problem technique used for estimating the

underlying activity from EEG signals has several challenges due to the ill-posed and the ill-conditioned characteristics of the problem. To help coping with these problems, an infinity configuration of brain activity estimation is proposed to explain the measured EEG signals, and hence, the regularization solutions can be applied to overcome the aforementioned challenges.

Several brain mapping methods have been presented in the last two decades, some of them are based on estimation theory with probabilistic frameworks like the multiple sparse priors MSP [1] and the dynamic multi-model source localization method DYNAMO [2]. Other methods are based on regularized solutions like minimum norm estimation (MNE), weighted minimum norm estimation (WMNE), low resolution tomography (LORETA), iterative regularization algorithm (IRA) and non-linear regularized observer (NLO) [3–7]. The NLO method involves a physiological model that represents the evolution of the activity in the brain. However, this method has a high dependence on the model parameters and these values change between subjects and sessions[7].

The Extended Kalman Filter (EKF) is a widely used estimator in non-linear processes. Due to the non-linear properties of EEG signals, the EKF can be a suitable estimator for identifying parameters in EEG data. Some applications of EKF to EEG and MEG signals have been reported for tracking the dipole source location[8], inverse problem solution and source estimation[2], and for noise reduction and filtering in [9]. This paper considers the implementation of an EKF for the step of model parameter estimation to create a dynamical non-linear regularized observer -DYNLO, to improve the brain mapping solution. The results of the implementation are evaluated comparing the EKF estimated EEG over a dataset of P300 visual evoked potentials VEP using MSP and NLO methods with LS parameter estimation.

2 Materials and Methods

2.1 EEG Forward model

The equation for relating the EEG signals measured in the scalp with the brain activity is known as the EEG forward problem, and it can be represented as shown in equation 1

$$\boldsymbol{y}_k = \boldsymbol{M}\boldsymbol{x}_k + \varepsilon_k \tag{1}$$

Where $\boldsymbol{y}_k \in \mathbb{R}^{d\times N}$ contains the EEG signals of d number of electrodes and N number of samples, $\boldsymbol{x}_k \in \mathbb{R}^{n\times N}$ represents the source activity inside the brain that produces the measured electrical impulses. n is the number of distributed sources considered in the brain. For relating the measured EEG $\boldsymbol{y}_k$ and the neural activity $\boldsymbol{x}_k$, the lead field matrix $\boldsymbol{M} \in \mathbb{R}^{d\times n}$ is introduced, this matrix is obtained from magnetic resonance images (MRI) and numerical methods e.g. Finite Element Method (FEM) or Boundary Element Method (BEM), which usually involves the skin, skull, cerebrospinal fluids (CSF) and brain matter to establish the position of sources and their relationship with electrodes. In

addition, a white noise with zero mean and C_ε covariance is considered. The subscript k represents the time instant of the sampled data.

2.2 Non-Linear Brain Activity Model

The activity in the brain exhibits a highly non-linear behaviour and can be viewed as a non-linear dynamical system as stated in [10] where the evolution of the activity considers previous samples as expressed in the following equation

$$\boldsymbol{x}_k = a_1\boldsymbol{x}_{k-1} + a_2\boldsymbol{x}_{k-2} + a_3\boldsymbol{x}_{k-\tau} + a_4\boldsymbol{x}_{k-2}^{\circ 2} + a_5\boldsymbol{x}_{k-2}^{\circ 3} + \boldsymbol{\eta}_k \tag{2}$$

The terms $\boldsymbol{x}_k^{\circ 2}$ and $\boldsymbol{x}_k^{\circ 3}$ represent the Hadamard power of $\boldsymbol{x}_k$ and a_i terms are the model parameter of the non-linear representation. Equation 2 shows that the actual activity depends of $i-th$ model parameters and on the previously sampled data $\boldsymbol{x}_{k-1}$, $\boldsymbol{x}_{k-2}$ and $\boldsymbol{x}_{k-\tau}$, where the $\tau-th$ sample is a feedback due to the activity of nearby neurons and depends on the sampling frequency of the EEG data. $\boldsymbol{\eta}_k$ is the noise in the activity, which is considered to follow a normal distribution with zero mean and covariance C_η. To simplify the notation, the equation 2 can be represented as a multiplication of the matrix $\boldsymbol{G}_k$ with $\boldsymbol{\omega}_k$, as shown below

$$\boldsymbol{x}_k = \boldsymbol{G}_k\boldsymbol{\omega}_k + \boldsymbol{\eta}_k \tag{3}$$

Where the parameters a_i are represented in a vector $\boldsymbol{\omega}_k$ denominated model parameter vector as in equation 4 and the temporal activity matrix $\boldsymbol{G}_k$ can be formed by the concatenation of the activity in previously sampled data as in equation 5.

$$\boldsymbol{\omega}_k = [a_1 \;\; a_2 \;\; a_3 \;\; a_4 \;\; a_5]^T \tag{4}$$

$$\boldsymbol{G}_k = [\hat{\boldsymbol{x}}_{k-1} \quad \hat{\boldsymbol{x}}_{k-2} \quad \hat{\boldsymbol{x}}_{k-\tau} \quad \hat{\boldsymbol{x}}_{k-2}^{\circ 2} \quad \hat{\boldsymbol{x}}_{k-2}^{\circ 3}] \tag{5}$$

2.3 Extended Kalman Filter for Model Parameter Estimation

The non-linear model parameter vector $\boldsymbol{\omega}_k$ that represents the dynamical behavior of the brain activity can be estimated using the EKF, where two standard Kalman filter steps are developed: the prediction and the correction steps. Initially in the prediction step, the *a priori* information is calculated in each instance k using the following equations

$$\hat{\boldsymbol{\omega}}_{\bar{k}} = \hat{\boldsymbol{\omega}}_{k-1} \tag{6}$$

$$\boldsymbol{P}_{\omega_k}^{-} = \boldsymbol{P}_{\omega_{k-1}} + \boldsymbol{R}_{k-1}^{r} \tag{7}$$

Where the term $\boldsymbol{P}_{\omega_k^-}$ is the *a priori* predicted covariance of model parameters, $\boldsymbol{\omega}_k^-$ is the *a priori* predicted model parameters, $\boldsymbol{P}_{\omega_{k-1}}$ is the predicted covariance in the previous sample, and $\boldsymbol{R}_{k-1}^r$ is a diagonal matrix called the innovation covariance and is defined as shown below.

$$\boldsymbol{R}_{k-1}^r = (\gamma^{-1} - 1)\boldsymbol{P}_{\omega_{k-1}} \tag{8}$$

Being $\gamma^{-1} \in \mathbb{R}^{[0,1]}$ a forgetting factor that represents the dependence of previous information, e.g. when it value tends to zero, the estimation has a strong dependence of previous estimations. The EKF gain matrix $\boldsymbol{K}_{\omega_k}$ can be computed as it is shown in equation 9below

$$\boldsymbol{K}_{\omega_k} = \boldsymbol{P}_{\omega_k^-}\boldsymbol{G}_k^T\boldsymbol{M}^T(\boldsymbol{G}_k\boldsymbol{M}\boldsymbol{P}_{\omega_k^-}\boldsymbol{G}_k^T\boldsymbol{M}^T + \boldsymbol{R}^e)^{-1} \tag{9}$$

The correction step allows to estimate the set of parameters $\hat{\boldsymbol{\omega}}_k$ and update the covariance of the parameters $\boldsymbol{P}_{\omega_k}$ using following equations 10 and 11.

$$\hat{\boldsymbol{\omega}}_k = \boldsymbol{\omega}_k^- + \boldsymbol{K}_{\omega_k}(\boldsymbol{y}_k - \boldsymbol{M}\boldsymbol{G}_k\hat{\boldsymbol{\omega}}_{k-1}) \tag{10}$$

$$\boldsymbol{P}_{\omega_k} = (\boldsymbol{I} - \boldsymbol{K}_{\omega_k}\boldsymbol{M}\boldsymbol{G}_k)\boldsymbol{P}_{\omega_k^-} \tag{11}$$

2.4 Non-Linear Regularized Observer

The non-linear regularized observer is defined by equation 12, where the inverse problem can be addressed as an optimization problem with constrains based on l_2 norm. The cost function is formed by three terms, where the first term represents the basic inverse solution with least squares; adding the second term, the solution involves a spatial constraint like in brain mapping methods MNE and LORETA presented in [5] and [6] respectively. The third term considers the time evolution of the activity and is treated as a temporal constraint as presented in [3] and [7]. The minimization problem involves the non-linear model, taking into account the activity in previously sampled data as shown in equations 2 to 5.

$$J = ||\boldsymbol{M}\boldsymbol{x}_k - \boldsymbol{y}_k||_2^2 + \rho_k^2||\boldsymbol{x}_k||_2^2 + \lambda_k^2||\boldsymbol{x}_k - \boldsymbol{G}_k\boldsymbol{\omega}_k||_2^2 \tag{12}$$

The variable ρ_k is the spatial regularization parameter and λ_k is the temporal regularization parameter. The estimation of the activity can be performed by equation 13, where the adaptive solution depends on the model parameter estimated with the EKF.

$$\hat{\boldsymbol{x}}_{k(\rho_k,\lambda_k,\hat{\boldsymbol{\omega}}_k)} = (\boldsymbol{M}^T\boldsymbol{M} + \rho_k^2\boldsymbol{I} + \lambda_k^2\boldsymbol{I})^{-1}(\boldsymbol{M}^T\boldsymbol{y}_k + \lambda_k^2\boldsymbol{G}_k\hat{\boldsymbol{\omega}}_k) \tag{13}$$

The lead field matrix M can be decomposed by singular values decomposition (SVD), where M can be represented by $M = USV^T$. By applying SVD of M on equation 13 it is possible to reduce the computational cost to estimate the activity, especially when the inverse of $(\boldsymbol{M}^T\boldsymbol{M} + \rho_k^2\boldsymbol{I} + \lambda_k^2\boldsymbol{I})$ in equation 13 is computed. The estimated neural activity $\hat{\boldsymbol{x}}$ involving the M SVD is shown in equation 14

$$\hat{\boldsymbol{x}}_{k(\rho_k,\lambda_k,\hat{\boldsymbol{\omega}}_k)} = \boldsymbol{V}(\boldsymbol{S}^2 + \rho_k^2\boldsymbol{I} + \lambda_k^2\boldsymbol{I})^{-1}\boldsymbol{V}^T(\boldsymbol{M}^T\boldsymbol{y}_k + \lambda_k^2\boldsymbol{G}_k\boldsymbol{\omega}_k) \tag{14}$$

3 Experimental Framework

For evaluating the proposed method, a dataset of P300 visual evoked potentials described in [11] was used. The protocol of the records consisted on six images displayed in a screen, which were flashed in random sequences with a duration of 100ms with a resting time of 300ms in between images. The subjects of this experiment were requested to count the times that a specific image appeared. The EEG signals from 8 subjects (four of them with neurological deficit called dysarthria or hypophonia) were recorded from 32 channels localized according to the 10-20 international system with a sample rate of 2048 Hz.

A head model is required for solving the inverse problem, therefore, we use a realistic brain model with $n = 8196$ distributed sources in the cortical surface. This model was computed with 70 electrodes on the scalp using the 10-10 system layout. The used model corresponds to the first subject of the dataset presented in [12]. The head model has 30 common electrodes with the EEG, hence, the distributed model was reduced to 30 according to the 10-20 system used in the EEG dataset. In addition, the EEG signals were organized to coincide with the channels' positions of the brain model.

Figure 1 shows the 30 electrodes and their distribution according to the 10-20 layout used in the EEG recordings. It additionally shows the 8196 distributed sources and how the electrodes are located in the scalp around the brain. The procedure followed for processing the data of each subject is explained by the next steps:

- *pre-processing:* The average signal from the two mastoid electrodes was used for referencing each one of the channels. In addition, the EEG channels were organized according to the head model order for electrodes, where the two electrodes Fp1 and Fp2 from dataset were discarded, because the used head model does not consider them in the forward model.
- *Inverse Solution:* The EKF is iteratively used to estimate the model parameters $\hat{\boldsymbol{\omega}}_k$ for the NLO method (DYNLO). NLO with LS and MSP methods were used for estimating the neural activity $\hat{\boldsymbol{x}}_k$, where the activity for each one of the 8196 distributed sources were found.
- *Forward Problem:* The EEG signals were estimated using the following equation, similar to equation 1.

$$\hat{\boldsymbol{y}}_k = \boldsymbol{M}\hat{\boldsymbol{x}}_k \tag{15}$$

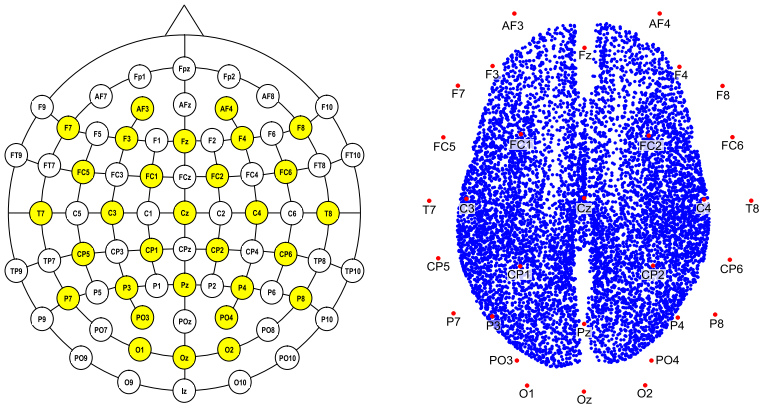

Fig. 1: Left: Head model electrodes layout according to 10-10 system and 30 electrodes (yellow) used under 10-20 layout. Right: Brain model with $n = 8196$ distributed sources (blue) and the 30 electrodes position (red)

– *Evaluation:* The estimated EEG signals using DYNLO, NLO-LS and MSP, were computed and compared with the original EEG signals used for the source estimation procedure. Two performance measurements were assessed: the relative error and the correlation coefficient shown in equations 16 and 17 respectively. These measurements were calculated for the 192 available runs.

$$\varepsilon_r = \frac{||\hat{\boldsymbol{y}}_k - \boldsymbol{y}_k||_2^2}{||\boldsymbol{y}_k||_2^2} \tag{16}$$

In addition, the correlation coefficient was calculated for evaluating the similarity between the estimated signal and the original referenced EEG. To compute the variable, the following equation is used:

$$C_c = \frac{1}{N-1} \sum_{k=1}^{N} \left(\frac{\boldsymbol{y}_k - \mu_{y_k}}{\sigma_{y_k}} \right) \left(\frac{\hat{\boldsymbol{y}}_k - \mu_{\hat{y}_k}}{\sigma_{\hat{y}_k}} \right) \tag{17}$$

Where the term μ and σ represent the mean and standard deviation respectively, being N the number of samples of y_k.

4 Results and Discussion

Figure 2 depicts the mean and the standard deviation of the relative error for the 192 runs with each one of the three methods. The mean of the relative errors were $\varepsilon_{r(MSP)} = 0,4459$, $\varepsilon_{r(NLO-LS)} = 0,1446$ and $\varepsilon_{r(DYNLO)} = 0,01271$. The lowest value of relative error was obtained when using DYNLO. In addition, the standard deviation was the lowest with DYNLO.

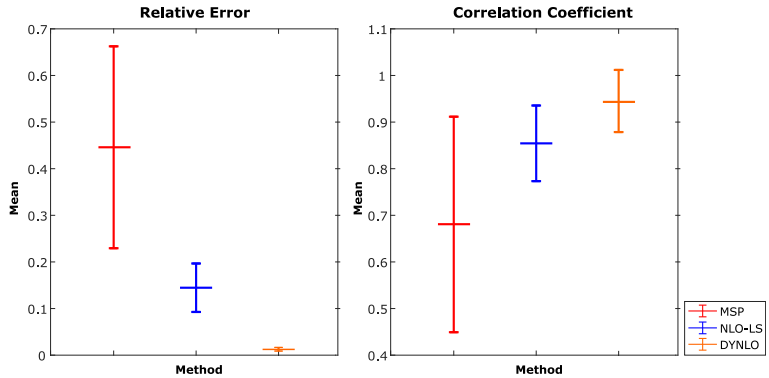

Fig. 2: Performance measurements over 192 runs of EEG data. Left: Mean and standard deviation of Relative error. Right: Mean and standard deviation of Correlation Coefficient

Additionally, figure 2 also shows the mean and the standard deviation of the correlation coefficient for the 192 runs with each one of the three methods. The mean of the correlation coefficients were $C_{c(MSP)} = 0,6803$, $C_{c(LS)} = 0,8544$ and $C_{c(EKF)} = 0,9459$. Considering that in this case a higher value of correlation is desired, the DYNLO has obtained the best performance correlation and standard deviation.

The estimated EEG signal for a single channel with each one of the methods and the original EEG signal are shown in figure 3. This figure shows that the DYNLO has the best fitting with the original EEG signal compared to NLO-LS and MSP. It is also evident in the lower plot that as time passes, the fitting is improving. In addition, it is noticeable that DYNLO has a good estimation of the signal amplitude, where NLO-LS and MSP present a higher difference.

Figure 4 shows the time evolution of the estimated model parameters using the EKF and LS for one of the runs, where the model values describe an asymptotic behavior. However, the EKF stabilizes the parameters faster than LS, situation that translates in a better performance in the correlation coefficient and the relative error. Furthermore, as stated in [7], the model parameters depend of the sampling frequency and the type of activity to be analyzed. i.e normal activity or seizure. In the case of the EEG dataset used in this study, the activity is considered normal and the sampling frequency is $2048Hz$. Therefore, the parameters can be calculated according to [7], where their values of the dataset frequency are presented in table 1. The table also includes the mean parameters of the estimations with EKF and LS methods.

When evaluating and comparing the computational costs of the two the iterative methods, DYNLO and NLO-LS, the computational time for estimating the model parameter vector $\hat{\boldsymbol{\omega}}_k$ using EKF in DYNLO is $0.835ms$ per sample, meanwhile, with LS in NLO, the required time per sample is $1.494ms$. From these results it is seen a reduction of computational time by 45% in the calculation

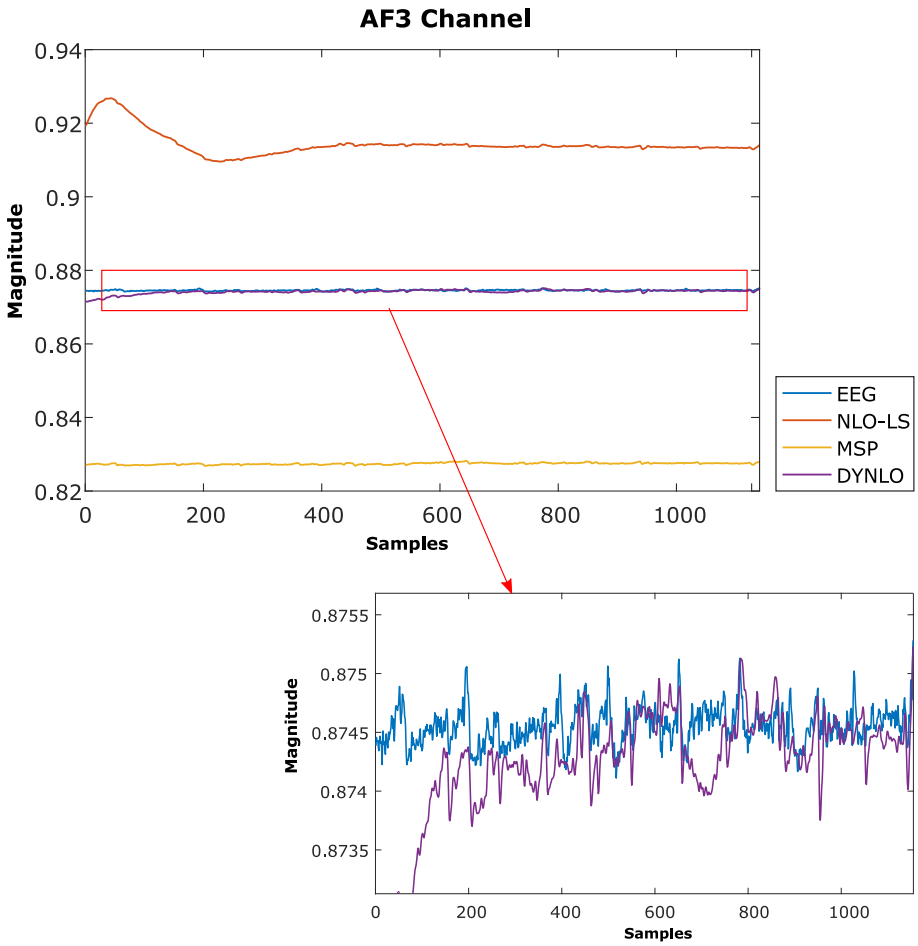

Fig. 3: Top: AF3 channel in measured EEG (blue), estimated with MSP (yellow), NLO-LS (red) and DYNLO (purple). Bottom: zoom of estimated AF3 channel with NLO EKF and original EEG

Table 1: 192 runs mean parameters estimated with EKF and LS and static NLO model parameter values

Method / Parameters	a_1	a_2	a_3	a_4	a_5
Static Parameters	1.9023	-0.9100	0.0067	1.1921e-04	-2.3842e-05
EKF	1.6477	-0,6472	-0.0004717	-1.2045e-06	1.4701-07
LS	0.5994	0.5637	-0.003596	-0.004754	0.002082

of $\hat{\omega}_k$. The time measurements where taken in a computer with the following characteristics: RAM 16GB , processor Core i7-4790, OS windows 10, 64-bit and executing the algorithms in Matlab® 2016b.

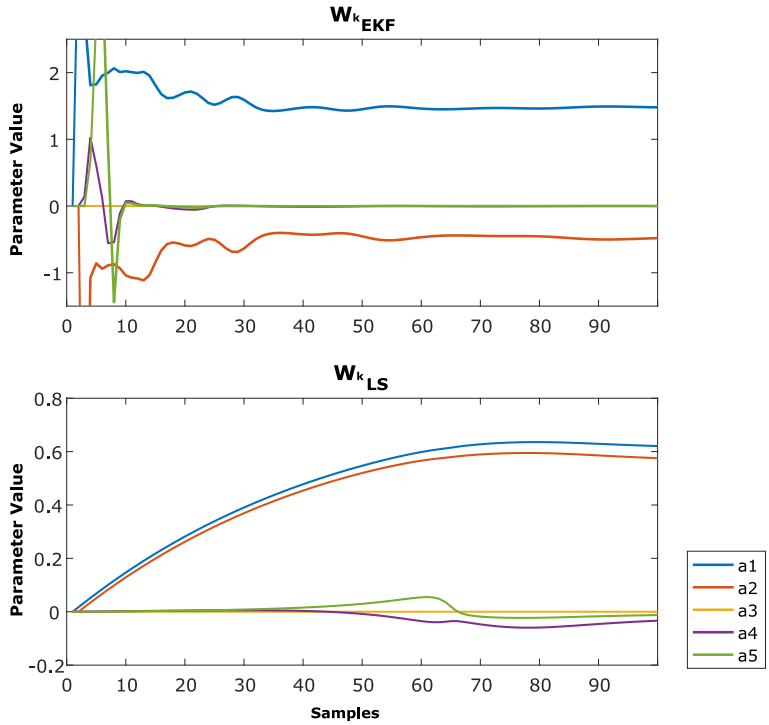

Fig. 4: Evolution of model parameter estimation by EKF in DYNLO (Top) and LS in NLO-LS(Bottom)

5 Conclusions and future work

The estimation of EEG signal parameters using EKF improves the brain activity estimation with NLO. A much better performance in the correlation between signals and a lower relative error were obtained with the DYNLO. In addition to these advantages in performance, the computational time was lower when using the EKF, which is a desirable feature to enable faster results in clinical analysis and essential for the use of brain mapping techniques in brain computer interfaces (BCI).

According to the results presented in this paper, the DYNLO approach provides faster brain mapping solutions which can be useful for real-time applications to study brain disorders/diseases, emotions, and memory processing evoked responses.

Generally, brain mapping methods require the information of high number of channels, which will result in high computational times. Nevertheless, the computational time and the response time towards real-time applications, could be improved by reducing the number of electrodes and using a lower sampling frequency. New experiments are currently being performed with the aforemen-

tioned reduction of channels and sampling frequency, and will be reported in the near future.

Acknowledgment

This work was carried out under the funding of Norwegian University of Science and Technology NTNU project "David and Goliath: single-channel EEG unravels its power through adaptive signal analysis" and the Departamento Administrativo Nacional de Ciencia, Tecnología e Innovación (Colciencias). Research project: 111077757982 "Sistema de identificación de fuentes epileptogénicas basado en medidas de conectividad funcional usando registros electroencefalográficos e imágenes de resonancia magnética en pacientes con epilepsia refractaria: apoyo a la cirugía resectiva".

References

1. Karl Friston, Lee Harrison, Jean Daunizeau, Stefan Kiebel, Christophe Phillips, Nelson Trujillo-Barreto, Richard Henson, Guillaume Flandin, and Jérémie Mattout. Multiple sparse priors for the M/EEG inverse problem. *NeuroImage*, 39(3):1104–1120, 2008.
2. Javier M. Antelis and Javier Minguez. Dynamo: Concurrent dynamic multi-model source localization method for eeg and/or meg. *Journal of Neuroscience Methods*, 212(1):28 – 42, 2013.
3. E. Giraldo-Suarez, J. D. Martinez-Vargas, and G. Castellanos-Dominguez. Reconstruction of Neural Activity from EEG Data Using Dynamic Spatiotemporal Constraints. *International Journal of Neural Systems*, 26(07):1650026, 2016.
4. Roberta Grech, Tracey Cassar, Joseph Muscat, Kenneth P Camilleri, Simon G Fabri, Michalis Zervakis, Petros Xanthopoulos, Vangelis Sakkalis, and Bart Vanrumste. Review on solving the inverse problem in EEG source analysis. *Journal of NeuroEngineering and Rehabilitation*, 5, 2008.
5. Olaf Hauk. Keep it simple: A case for using classical minimum norm estimation in the analysis of EEG and MEG data. *NeuroImage*, 21(4):1612–1621, 2004.
6. Roberto Domingo Pascual-Marqui. Review of Methods for Solving the {EEG} Inverse Problem. *Intl.\ J.\ Biomagn.*, 1(1):75–86, 1999.
7. Andrés Felipe Soler, Pablo Andrés Muñoz-Gutiérrez, and Eduardo Giraldo. Regularized state observers for source activity estimation. In Shouyi Wang, Vicky Yamamoto, Jianzhong Su, Yang Yang, Erick Jones, Leon Iasemidis, and Tom Mitchell, editors, *Brain Informatics*, pages 195–204, Cham, 2018. Springer International Publishing.
8. Y. Yao and A. L. Swindlehurst. Tracking single dynamic meg dipole sources using the projected extended kalman filter. In *2011 Annual International Conference of the IEEE Engineering in Medicine and Biology Society*, pages 4365–4368, Aug 2011.
9. J. Walters-Williams and Yan Li. Comparison of extended and unscented kalman filters applied to eeg signals. In *IEEE/ICME International Conference on Complex Medical Engineering*, pages 45–51, July 2010.
10. A. F. Soler and E. Giraldo. An adaptive nonlinear regularized observer for neural activity reconstruction. In *2018 IEEE ANDESCON*, pages 1–5, Aug 2018.

11. Ulrich Hoffmann, Jean-Marc Vesin, Touradj Ebrahimi, and Karin Diserens. An efficient p300-based braincomputer interface for disabled subjects. *Journal of Neuroscience Methods*, 167(1):115 – 125, 2008. Brain-Computer Interfaces (BCIs).
12. Richard N. Henson, Daniel G. Wakeman, Vladimir Litvak, and Karl J. Friston. A Parametric Empirical Bayesian Framework for the EEG/MEG Inverse Problem: Generative Models for Multi-Subject and Multi-Modal Integration. *Frontiers in Human Neuroscience*, 5(August):1–16, 2011.